Biogeosciences, 14, 5003–5014, 2017
https://doi.org/10.5194/bg-14-5003-2017

Biogeosciences Open Access EGU

Regional-scale lateral carbon transport and CO_2 evasion in temperate stream catchments

Katrin Magin, Celia Somlai-Haase, Ralf B. Schäfer, and Andreas Lorke

Institute for Environmental Sciences, University of Koblenz-Landau, Fortstr. 7, 76829 Landau, Germany

Correspondence to: Katrin Magin (magi6618@uni-landau.de)

Received: 23 January 2017 – Discussion started: 13 February 2017
Revised: 11 September 2017 – Accepted: 26 September 2017 – Published: 8 November 2017

Abstract. Inland waters play an important role in regional to global-scale carbon cycling by transporting, processing and emitting substantial amounts of carbon, which originate mainly from their catchments. In this study, we analyzed the relationship between terrestrial net primary production (NPP) and the rate at which carbon is exported from the catchments in a temperate stream network. The analysis included more than 200 catchment areas in southwest Germany, ranging in size from 0.8 to 889 km^2 for which CO_2 evasion from stream surfaces and downstream transport with stream discharge were estimated from water quality monitoring data, while NPP in the catchments was obtained from a global data set based on remote sensing. We found that on average 13.9 g C m^{-2} yr^{-1} (corresponding to 2.7 % of terrestrial NPP) are exported from the catchments by streams and rivers, in which both CO_2 evasion and downstream transport contributed about equally to this flux. The average carbon fluxes in the catchments of the study area resembled global and large-scale zonal mean values in many respects, including NPP, stream evasion and the carbon export per catchment area in the fluvial network. A review of existing studies on aquatic–terrestrial coupling in the carbon cycle suggests that the carbon export per catchment area varies in a relatively narrow range, despite a broad range of different spatial scales and hydrological characteristics of the study regions.

1 Introduction

Inland waters represent an important component of the global carbon cycle by transporting, storing and processing significant amounts of organic and inorganic carbon (C) and by emitting substantial amounts of carbon dioxide (CO_2) to the atmosphere (Cole et al., 2007; Aufdenkampe et al., 2011). Globally about 0.32 to 0.8 Pg C is emitted per year as CO_2 from lakes and reservoirs (Raymond et al., 2013; Barros et al., 2011). For streams and rivers, the global estimates range from 0.35 to 1.8 Pg C yr^{-1} (Raymond et al., 2013; Cole et al., 2007), where the lower estimates can be considered as conservative because they omit CO_2 emissions from small headwater streams. In 2015 global CO_2 evasion from rivers and streams was estimated at 0.65 Pg C yr^{-1} (Lauerwald et al., 2015). Comparable amounts of C are discharged into the oceans by the world's rivers (0.9 Pg C yr^{-1}) and stored in aquatic sediments (0.6 Pg C yr^{-1}) (Tranvik et al., 2009). In total, evasion, discharge and storage of C in inland waters have been estimated to account for about 4 % of global terrestrial net primary production (NPP; Raymond et al., 2013) or 50–70 % of the total terrestrial net ecosystem production (NEP; Cole et al., 2007). A recent continental-scale analysis, which combined terrestrial productivity estimates from a suite of biogeochemical models with estimates of the total aquatic C yield for the conterminous United States (Butman et al., 2015), resulted in mean C export rates from terrestrial into freshwater systems of corresponding to 4 % of NPP and 27 % of NEP. These estimates varied by a factor of 4 across 18 hydrological units with surface areas between 10^5 and 10^6 km^2.

The substantial lateral and vertical transport of terrestrial-derived C in inland waters is currently not accounted for in most bottom-up estimates of the terrestrial uptake rate of atmospheric CO_2 (Battin et al., 2009) and results in high uncertainties in regional-scale C budgets and predictions of their response to climate change, land use and water management. Only few studies have quantified C fluxes and pools including inland waters at the regional scale (10^3–10^4 km^2) (Chris-

tensen et al., 2007; Buffam et al., 2011; Jonsson et al., 2007; Maberly et al., 2013) or for small (1–10 km^2) catchments (Leach et al., 2016; Shibata et al., 2005; Billett et al., 2004). The majority of existing regional-scale studies on terrestrial–aquatic C fluxes are from the boreal zone and are characterized by a relatively large fractional surface area covered by inland waters, a high abundance of lakes and high fluvial loads of dissolved organic carbon (DOC). Landscapes in the temperate zone can differ in all these aspects, potentially resulting in differences in the relative importance of aquatic C-fluxes and flux paths (storage, evasion and discharge) in regional-scale C budgets. In this study, we provide a representative investigation of a temperate watershed to improve the understanding of the role of temperate inland water bodies in the regional and global C-cycles. We analyzed the relationship between terrestrial NPP and CO_2 evasion and C discharge for more than 200 catchments in southwest Germany. The stream-dominated catchments range in size from 0.8 to 889 km^2 and are characterized by a relatively small fraction of surface water coverage (< 0.5 % of the land surface area). In contrast to studies from the boreal zone, the fluvial C load is dominated by dissolved inorganic carbon (DIC). Estimates of aquatic C-export from the catchments were obtained from water quality and hydrological monitoring data and were related to terrestrial NPP derived from MODIS satellite data. The scale dependence of aquatic C-fluxes in relation to NPP is analyzed by grouping the data according to Strahler stream order (Strahler, 1957). By comparing our results to a variety of published studies, we finally discuss the magnitude and the relative importance of different fluvial flux paths in regional-scale C budgets in different landscapes and climatic zones.

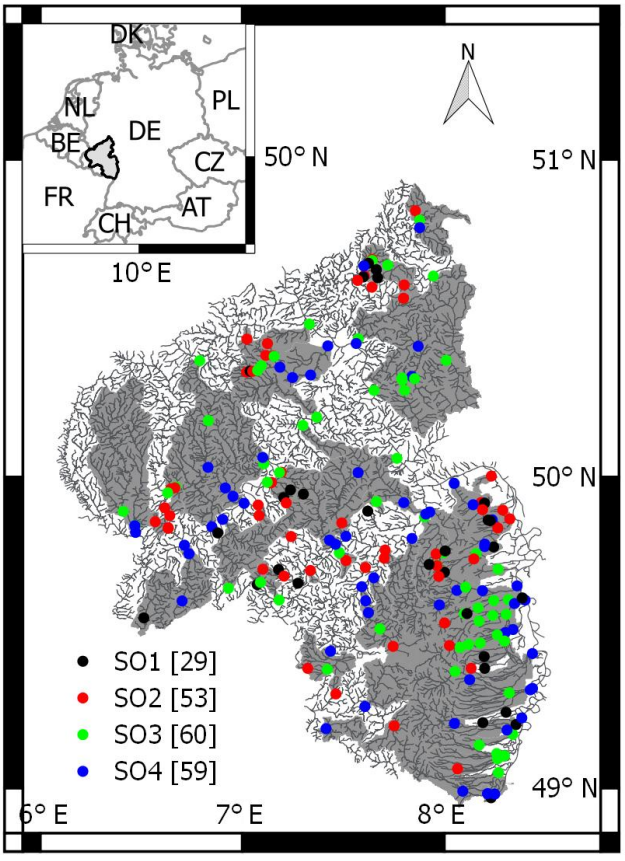

Figure 1. Map of the stream network (black lines) within the state borders of Rhineland-Palatinate in southwest Germany. The inset map in the upper left corner indicates the location of the study region in central Europe. Filled circles mark the positions of sampling sites with color indicating stream order (SO1–SO4; the numbers in brackets in the legend are the respective number of sampling sites). The catchment areas of the sampling sites are marked in grey.

2 Materials and Methods

2.1 Study area and hydrological characteristics

The study area encompasses large parts of the federal state of Rhineland-Palatinate (RLP) in southwest Germany (Fig. 1). The average altitude is 323 m (48–803 m) and the mean annual temperature and precipitation varied between 5.8 and 12.2 °C and 244 and 1576 mm, respectively, during the time period between 1991 and 2011 at the 37 meteorological stations operated by the state of RLP (http://www.wetter.rlp.de/). The dominant land covers in the study area are woodland (41 %, mainly mixed and broad-leaved forest), tilled land (37 %, mainly arable land and vineyards) and grassland (13 %, mainly pastures) (Corine land cover; EEA, 2006). The fraction of peatland in the study area is small (0.95 km^2; 0.009 % of the study area) and 16 % of the study area contains carbonate bedrock.

Most of the rivers in RLP are part of the catchment area of the Rhine River. Other large rivers in the state are the Mosel, Lahn, Saar and Nahe. The upland regions of RLP are the sources of many small, steep and highly turbulent streams with gravel beds (MULEWF, 2015). Lakes in RLP are small with a total area of approximately 40 km^2 (Statistisches Landesamt Rheinland-Pfalz, 2014) and were omitted from the analysis. The river network has a total length of 15 800 km and consists of stream orders (Strahler, 1957) between 1 and 7. A catchment map of RLP, consisting of subcatchments of 7729 river segments was provided by the state ministry (MULEWF, 2013), where a river segment refers to the section between a source and the first junction with another river or between two junctions with other rivers. All subsequent analyses were conducted separately for each stream order and streams of Strahler order greater than 4 were omitted from the analysis because of the limited sample size with only few catchments available. Moreover, we omitted streams for which parts of the catchment area were outside of the study area. Overall, 3377, 1619, 861 and 453 stream segments were retained for the analysis for Strahler orders of 1 to 4, respectively. Annual mean discharge and length of the

river segments were obtained from digital maps provided by the state ministry (MULEWF, 2013).

2.2 Aquatic C concentrations

DIC concentrations and partial pressure of dissolved CO_2 (pCO_2) in stream water were estimated from governmental water quality monitoring data which were acquired according to DIN EN ISO norms (DIN EN ISO 10523:2012-04; DIN EN ISO 9963-1:1996-02; DIN EN ISO 9963-2:1996-02). The data include measurements of alkalinity, pH and temperature which were conducted between 1977 and 2011 (MULEWF, 2013). Sampling intervals differed between the sites and water sampling was conducted irregularly with respect to year and season. To exclude a potential bias resulting from the seasonality of DIC concentrations on the analysis, we only considered river segments for which at least one measurement was available for each season (spring, summer, autumn and winter). From these measurements, pCO_2 and DIC concentrations were estimated using chemical equilibrium calculations with the software PHREEQC (version 2) (Parkhurst and Appelo, 1999). For 201 river segments with seasonally resolved measurements, we first computed seasonal mean pCO_2 and DIC concentrations, which subsequently were aggregated to annual mean values averaged over the entire sampling period:

$$\overline{pCO_{2\text{annual}}} = (\overline{pCO_{2\text{spring}}} + \overline{pCO_{2\text{summer}}} + \overline{pCO_{2\text{autumn}}} + \overline{pCO_{2\text{winter}}})/4. \quad (1)$$

Measurements of dissolved and total organic C (TOC) were available only for 64 of these sampling sites.

2.3 Estimation of lateral DIC export and catchment scale CO_2 evasion

The lateral export of DIC and the total CO_2 evasion from the upstream network were calculated for each of the 201 sampling sites with seasonally averaged concentration estimates. The lateral DIC export from the corresponding catchments was calculated as the product of the mean DIC concentration and discharge. CO_2 evasion from the stream network upstream of each sampling site was estimated by interpolating pCO_2 for all river segments without direct measurements by averaging the mean concentrations by stream order and assigning them to all stream segments of the river network (Butman and Raymond, 2011). Stream width (w, in m), depth (d, in m) and flow velocity (v, in m s^{-1}) were estimated from the discharge (Q, in m^3 s^{-1}) using the following empirical equations (Leopold and Maddock Jr, 1953):

$$w = a \cdot Q^b, \quad (2)$$
$$d = c \cdot Q^d,$$
$$v = e \cdot Q^f.$$

For the hydraulic geometry exponents and coefficients, the values from Raymond et al. (2012) were used ($b = 0.42$, $d = 0.29$, $f = 0.29$, $a = 12.88$, $c = 0.4$ and $e = 0.19$).

The water surface area (A, in m^2) was calculated as the product of length and width of the river segments. The average slope for each segment was estimated from a digital elevation map (resolution 10 m) provided by the federal state of RLP (LVermGeoRP, 2012). Zhang and Montgomery (1994) investigated the effect of digital elevation model (DEM) resolution on the slope calculation and performance in hydrological models for spatial resolutions between 2 and 90 m. They found that while a 10 m grid is a significant improvement over 30 m or coarser grid sizes, finer grid sizes provide relatively little additional resolution. Thus, a 10 m grid size represents a reasonable tradeoff between increasing spatial resolution and data handling requirements for modeling surface processes in many landscapes. The gas transfer velocity of CO_2 at 20 °C (k_{600}, in m d^{-1}) was calculated from slope (S) and flow velocity (v, in m s^{-1}) (Raymond et al., 2012).

$$k_{600} = S \cdot v \cdot 2841.6 + 2.03 \quad (3)$$

This gas transfer velocity was adjusted to the in situ temperature (k_T, in m d^{-1}) using the following equation:

$$k_T = k_{600} \cdot \left(\frac{Sc_T}{600}\right)^{-0.5}. \quad (4)$$

where Sc_T is the Schmidt number (ratio of the kinematic viscosity of water and the diffusion coefficient of dissolved CO_2) at the in situ temperature (Raymond et al., 2012). Finally the CO_2 flux (F_D, in g C m^{-2} yr^{-1}) for each stream segment was calculated as

$$F_D = k_T \cdot K_H \left(pCO_2 - pCO_{2,a}\right) \cdot M_C. \quad (5)$$

The partial pressure of CO_2 in the atmosphere ($pCO_{2,a}$) was considered as constant (390 ppm) and the Henry coefficient of CO_2 at in situ temperature (K_H, in mol L^{-1} atm^{-1}) was estimated using the relationship provided in Stumm and Morgan (1996). M_C is the molar mass of C (12 g mol^{-1}). Finally, the total CO_2 evasion was estimated by summing up the product of F_D with the corresponding water surface area for all stream segments located upstream of each individual sampling point.

2.4 Estimation of the catchment NPP

Average NPP in the catchment areas of the study sites were obtained from a global data set derived from the moderate

resolution imaging spectroradiometer (MODIS) observations of the earth observing system (EOS) satellites, which is available for the time period 2000 to 2013 with a spatial resolution of 30 arcsec ($\sim 1\,km^2$; Zhao et al., 2005). In this data set, NPP was estimated based on remote sensing observations of spectral reflectance, land cover and surface meteorology as described in detail by Running et al. (2004). We used mean NPP data (2000–2013) averaged over the catchment areas of the individual sampling sites.

2.5 Statistical analysis

Linear regressions (F test) were used to analyze the data. Group differences or correlations with $p<0.05$ were considered statistically significant. For the regression of total aquatic C-export rate and annual catchment NPP, data were log-transformed to correct for normal distribution. All statistical analyses were performed with R (R Development Core Team, 2011).

3 Results

3.1 Catchment characteristics and aquatic C load

The size of the analyzed catchment areas varied over 3 orders of magnitude (0.8 to 889 km^2) and the mean size increased from 9 km^2 for 1st order streams to 243 km^2 for streams of the order 4 (Table 1). Mean discharge and catchment area were linearly correlated ($r^2 = 0.74$, $p<0.001$). The runoff depth, i.e., the stream discharge divided by the catchment area, was relatively constant across stream orders with a mean value of 0.28 $m\,yr^{-1}$, corresponding to 35 % of the annual mean precipitation rate in the study area. The mean discharge increased more than 30-fold from 0.06 to 2.2 $m^3\,s^{-1}$ for 1st to 4th order streams, respectively. Similarly, the estimated water surface area increased with increasing stream order from 0.24 to 0.42 % of the corresponding catchment size (Table 1).

Individual estimates of the CO_2 partial pressure at the sampling sites varied between 145 and 7759 ppm. Only 1 % of the pCO_2 values were below the mean atmospheric value (390 ppm), indicating that the majority of the stream network was a source of atmospheric CO_2 in all seasons. The pCO_2 was higher in summer (mean ± SD: 2780 ± 2098 ppm) and autumn (mean ± SD: 2848 ± 2019 ppm) than in winter (mean ± SD: 2287 ± 1716 ppm) and spring (mean ± SD: 2172 ± 2343 ppm). The total mean value of pCO_2 was 2083 ppm and pCO_2 and DIC did not differ significantly among the different stream orders (pCO_2 : $p = 0.35$, DIC: $p = 0.56$). On average, DIC in the stream water was composed of 91.2 % bicarbonate, 0.4 % carbonate and 8.4 % CO_2.

The few available samples of DOC and TOC indicate that the organic C concentration was about 1 order of magnitude smaller than the inorganic C concentration (Table 1). There were no pronounced regional or temporal differences in organic C. Only a small fraction of TOC was in particulate form (on average 8.6 %) and TOC was linearly related to DIC, indicating that the organic load made up only 4 % of the total C load at the sampling sites (Fig. 2). The data are provided in the Supplement.

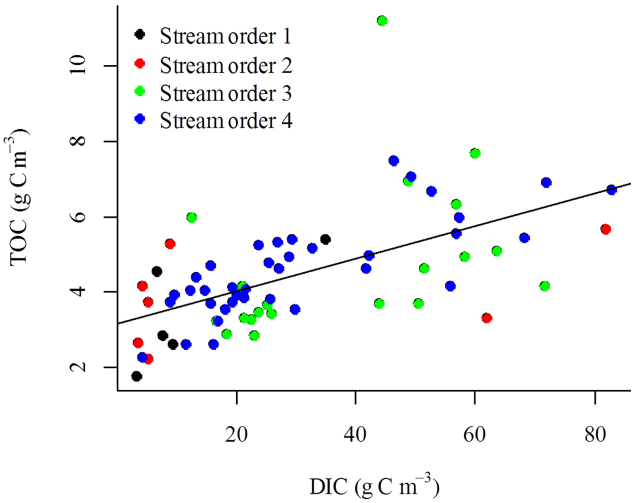

Figure 2. TOC versus DIC concentration. Different colors indicate sampling sites from different stream orders. The solid line shows the fitted linear regression model with TOC = 0.04 · DIC ($r^2 = 0.33$, $p<0.001$).

3.2 Catchment NPP and C budget

NPP increased linearly with catchment size ($r^2 = 0.98$, $p<0.001$), but the specific NPP, i.e., the total NPP within a catchment divided by catchment area, did not differ significantly ($p = 0.24$) among catchments of different stream orders. The smallest mean value and the largest variability of specific NPP (mean ± SD: 466 ± 127 $g\,C\,m^{-2}\,yr^{-1}$, range: 106 to 661 $g\,C\,m^{-2}\,yr^{-1}$) was observed among the small catchments of 1st order streams, while the variability was consistently smaller for higher stream orders (Table 2). The total average of terrestrial NPP in the study area was 515 ± 79 $g\,C\,m^{-2}\,yr^{-1}$ (mean ± SD).

In a simplified catchment-scale C balance, we consider the sum of the DIC discharge (DIC concentration multiplied by discharge) measured at each sampling site and the total CO_2 evasion from the upstream network as the total amount of C that is exported from the catchment area through the aquatic conduit. The total evasion was estimated by interpolation with stream-order specific pCO_2 values assigned to the complete stream network. Given the small number of available measurements, we neglect the fraction of organic C which is exported with stream discharge. As demonstrated above, TOC load is small in comparison to the DIC load (Fig. 2), resulting in a comparably small (< 4 %) error.

Table 1. Major hydrological characteristics, pCO_2, DIC and DOC concentrations averaged over stream orders (SO) and for all sampling sites (Total). All values are provided as mean ± SD (standard deviation) of the annual mean observations, ranges are given in brackets and n is the number of observations.

	SO 1	SO 2	SO 3	SO 4	Total
n	29	53	60	59	201
Catchment size (km^2)	9 ± 7 (1–35)	16 ± 9 (4–37)	87 ± 54 (9–298)	243 ± 140 (48–889)	103 ± 126 (1–889)
Water coverage (%)	0.24 ± 0.11 (0.05–0.43)	0.26 ± 0.09 (0.1–0.45)	0.36 ± 0.11 (0.09–0.6)	0.42 ± 0.13 (0.18–0.7)	0.33 ± 0.13 (0.05–0.7)
Discharge ($m^3\,s^{-1}$)	0.06 ± 0.05 (0.003–0.19)	0.15 ± 0.10 (0.01–0.36)	0.73 ± 0.63 (0.02–3.41)	2.20 ± 1.95 (0.22–12.22)	0.91 ± 1.41 (0.003–12.22)
Drainage rate ($m\,yr^{-1}$)	0.26 ± 0.17 (0.05–0.67)	0.29 ± 0.16 (0.06–0.66)	0.27 ± 0.17 (0.05–0.74)	0.30 ± 0.21 (0.06–1.20)	0.28 ± 0.18 (0.05–1.20)
pH	7.58 ± 0.61 (6.20–8.97)	7.70 ± 0.46 (6.30–8.60)	7.81 ± 0.37 (6.60–8.30)	7.75 ± 0.29 (6.91–8.30)	7.73 ± 0.42 (6.20–8.97)
Alkalinity ($mmol\,L^{-1}$)	3.08 ± 2.50 (0.08–7.58)	2.74 ± 2.58 (0.08–8.55)	2.77 ± 1.85 (0.14–9.88)	2.58 ± 1.73 (0.32–7.22)	2.75 ± 2.12 (0.08–9.88)
pCO_2 (ppm)	2597 ± 1496 (145–6706)	1819 ± 1095 (681–5338)	1992 ± 1327 (573–7627)	2162 ± 1302 (366–7759)	2083 ± 1303 (145–7759)
DIC ($g\,m^{-3}$)	38.8 ± 30.3 (3.4–93.1)	34.2 ± 31.1 (3.5–104.5)	34.6 ± 22.4 (3.1–119.6)	32.4 ± 21.0 (4.1–89.3)	34.5 ± 25.7 (3.1–119.6)
DOC ($g\,m^{-3}$)	3.54 ± 1.86 (2.2–6.7) ($n = 5$)	4.11 ± 0.73 (3.1–4.8) ($n = 4$)	4.17 ± 1.08 (2.6–7.1) ($n = 22$)	4.10 ± 1.24 (2.0–7.7) ($n = 33$)	4.08 ± 1.20 (2.0–7.7) ($n = 64$)

Table 2. Aquatic C-fluxes and terrestrial NPP in catchments drained by streams of different stream orders (SO) and for all sampling sites (Total). All values are mean ± standard deviation and ranges are given in brackets. The CO_2 flux from the water surface (first row) is expressed per square meter water surface area, while the remaining fluxes are expressed per square meter catchment area.

	SO 1	SO 2	SO 3	SO 4	Total
CO_2 flux from water surface ($g\,C\,m^{-2}\,yr^{-1}$)	2415 ± 2335 (-335–12 915)	1975 ± 1364 (418–7143)	1998 ± 1671 (704–11 016)	1928 ± 903 (851–5093)	2032 ± 1528 (-335–12 915)
Gas transfer velocity k_{600} ($m\,d^{-1}$)	7.04 ± 4.52 (2.16–20.57)	7.74 ± 3.78 (2.03–20.50)	5.86 ± 2.81 (2.03–15.55)	4.23 ± 0.96 (2.03–6.50)	6.05 ± 3.32 (2.03–20.57)
CO_2 evasion per catchment area ($g\,C\,m^{-2}\,yr^{-1}$)	5.9 ± 6.3 (-1.0–30.0)	5.2 ± 4.1 (0.7–19.2)	7.0 ± 6.6 (1.6–43.8)	8.0 ± 4.6 (3.0–23.0)	6.6 ± 5.5 (-1.0–43.8)
DIC discharge per catchment area ($g\,C\,m^{-2}\,yr^{-1}$)	6.2 ± 4.5 (1.6–25.8)	7.1 ± 6.1 (0.6–27.2)	7.7 ± 5.7 (1.6–35.5)	7.5 ± 4.7 (1.2–24.5)	7.3 ± 5.4 (0.6–35.5)
Total aquatic C-export per catchment area ($g\,C\,m^{-2}\,yr^{-1}$)	12.1 ± 6.9 (4.7–34.5)	12.3 ± 6.9 (1.5–29.6)	14.7 ± 10.8 (5.3–66.8)	15.5 ± 6.7 (7.0–33.8)	13.9 ± 8.3 (1.5–66.8)
NPP ($g\,C\,m^{-2}\,yr^{-1}$)	466 ± 127 (106–661)	536 ± 66 (251–644)	527 ± 57 (364–627)	508 ± 69 (330–618)	515 ± 79 (106–661)

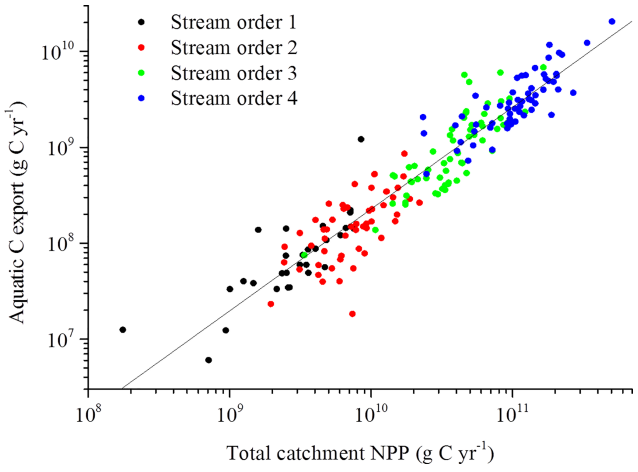

Figure 3. Annual rate of C export through the stream network versus terrestrial NPP in the catchment area. Different colors indicate sampling sites from different stream orders. The solid line shows the fitted linear regression model for the log-transformed data with $C\_export = 0.005 \cdot NPP^{1.06}$ ($r^2 = 0.89$, $p < 0.001$).

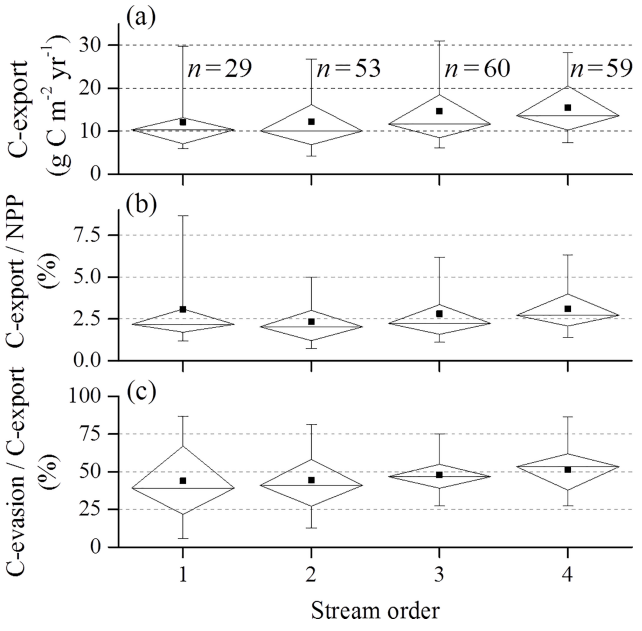

Figure 4. (a) Box plots of C export (sum of evasion and discharge) normalized by catchment area. **(b)** Box plots of the ratio of the total exported C and terrestrial NPP for different stream orders. **(c)** Box plots of the fraction of the total exported C which is emitted to the atmosphere from the stream network for each stream order. The boxes demarcate the 25th and 75th percentiles and the whiskers demarcate the 95 % confidence intervals. Median and mean values are marked as horizontal lines and square symbols, respectively. The sample numbers (n) provided in **(a)** apply to all panels.

The resulting CO_2 evasion rates decreased slightly, but not significantly ($p = 0.26$) for increasing stream orders with a total mean evasion rate of 2032 g C m^{-2} yr^{-1} (expressed as per unit water surface area; Table 2). The total aquatic evasion rate within catchments normalized by the size of the catchment increased significantly with stream order with a mean value of 6.6 g C m^{-2} yr^{-1} (Table 2).

The total aquatic C-export rate, i.e., the sum of evasion and DIC discharge, was strongly correlated with annual mean NPP averaged over the corresponding catchment area. Linear regression of the log-transformed data results in a power-law exponent of 1.06, indicating a nearly linear relationship (Fig. 3). As small streams of low stream order can be directly influenced by local peculiarities, the relationship is more variable for streams of Strahler order 1 and 2, while larger streams represent more average conditions over larger spatial scales with less variability. However, most of the correlation between the total aquatic C-export rate and the annual mean NPP can be attributed to their common linear-scale dependence.

After normalization with catchment area, the total aquatic C-export rate increased slightly with stream order (Fig. 4a). Also, the ratio of the C exported through the aquatic network (i.e., the sum of evasion and discharge) to the terrestrial NPP increased slightly, though not significantly ($p = 0.32$), from 2.18 % for 1st order streams to 2.72 % for stream order 4 (Fig. 4b). This increase was related to increasing rates of CO_2 evasion in streams of higher order and the contribution of evasion to the total C-export rate increased from 39 to 53 % (Fig. 4c). The increasing evasion is mainly caused by the increasing fractional water surface area for increasing stream orders (Table 1), because the CO_2 fluxes per water surface showed a rather opposing trend with decreasing fluxes for increasing stream orders (Table 2). On average, 1.31 % of the catchment NPP is emitted as CO_2 from the stream network and 1.49 % is discharged downstream (Table 2).

No regional (large-scale) pattern or gradients were observed in the spatial variation in catchment-scale NPP nor aquatic C-export (Fig. 5).

4 Discussion

4.1 Uncertainty analysis

Our estimates are subject to a number of uncertainties associated with sampling, interpolation and systematic errors including the neglect of C burial in sediments, C export and evasion as methane, and unresolved spatial and temporal variability.

According to Abril et al. (2015), high uncertainties of pCO_2 estimates from pH and alkalinity measurements occur at pH values < 7. In our study, only 7 % of the pH values were < 7. For pH > 7 the median and mean relative errors are 1 and 15%, respectively (Abril et al., 2015). Raymond et al. (2013) estimated uncertainties from comparisons of estimates obtained using approaches comparable to the present study with direct measurements of CO_2 concentration on

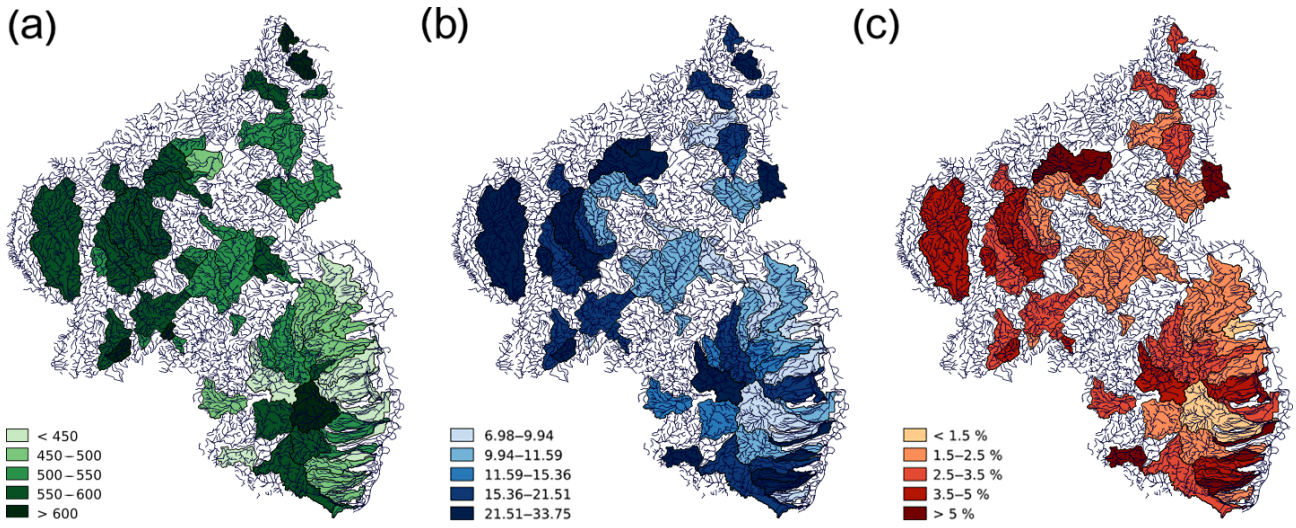

Figure 5. Map of 3rd and 4th order catchments showing **(a)** mean NPP ($g\,C\,m^{-2}\,yr^{-1}$), **(b)** aquatic export ($g\,C\,m^{-2}\,yr^{-1}$) and **(c)** ratio aquatic export/NPP (%).

streams. For a density of sampling locations of 0.02 sites per km^2 (corresponding to this study) they derived an uncertainty of 30 %. Similarly, Butman and Raymond (2011) estimated uncertainties of overall flux estimates of 33 %, based on Monte Carlo simulation of similar data for hydrographic units in the United States. However, we expect that these unbiased, i.e., randomly distributed, uncertainties did not affect the general results of our model.

While the riverine C concentrations were obtained from measurements that covered a time period from 1977 to 2011, the NPP data were available for the time period from 2000 to 2013. In boreal and subtropical rivers, an increasing per decade DIC export due to climate change and anthropogenic activities has been observed (Walvoord and Striegl, 2007; Raymond et al., 2008); therefore the different time periods covered by the two data sets might pose a problem. However, comparisons of DIC measurements in the study area between 1977–1999 and 2000–2011 did not show significant changes. Furthermore, the sampling frequency for DIC increased so that the majority of DIC measurements originated from the same time period as the NPP data.

The hydraulic geometry exponents and coefficients used in this study were derived from various data sets obtained in North America, not for central Europe. Unfortunately, we are not aware of a comparably extensive data set of hydraulic geometry data derived for European rivers. The coefficients have been applied in global studies before, e.g., Raymond et al. (2013). A comparison of hydraulic geometry coefficients derived from various data sets, including data from England, Australia and New Zealand, is presented in Butman and Raymond (2011), who estimated that the error associated with uncertainties of hydraulic geometry coefficients is rather small compared to uncertainties derived for C fluxes.

C burial in sediments was neglected in this study but can make a significant contribution to catchment-scale C balances. Estimates vary between 22 % at a global scale (Aufdenkampe et al., 2011), 14 % for the conterminous US (Butman et al., 2015) and 39 % for the Yellow River network (Ran et al., 2015). However, C storage in aquatic systems occurs mainly in lakes and reservoirs, which are virtually absent in the study area. Therefore we consider the bias caused by neglecting storage to be small in comparison to remaining uncertainties (30 %).

Similarly, the transport of C as methane was neglected because measurements of methane concentration or fluxes were not available for the study area. According to a recent meta-analysis, the dissolved methane concentration in headwater streams varies mainly between 0.1 and 1 $\mu mol\,L^{-1}$, with streams in temperate forests being at the lower end (Stanley et al., 2016). As the methane makes up only a small fraction of total C in comparison to the mean DIC concentration in the present study (500 $\mu mol\,L^{-1}$), it can be assumed that methane makes a rather small contribution to the catchment-scale C balance.

Since no time-resolved discharge data were available for the sampling sites, we cannot account for extreme events. Moreover, no information was available if the governmental monitoring included sampling during floods. Given the stochastic nature and short duration, we expect that such samples are at least underrepresented. Since it has been observed that high-discharge events can make a disproportionally high contribution to annual mean C export from catchments, we consider our estimates as a lower bound.

4.2 An average study region

The average C fluxes in the catchments of the study area resemble global and large-scale zonal mean estimates in many aspects. The mean atmospheric flux of CO_2 from the stream network of $2031 \pm 1527\,g\,C\,m^{-2}\,yr^{-1}$ is in close agreement with bulk estimates for streams and rivers in the temperate zone of $2630\,g\,C\,m^{-2}\,yr^{-1}$ (Aufdenkampe et al., 2011) and $2370\,g\,C\,m^{-2}\,yr^{-1}$ (Butman and Raymond, 2011). The fractional surface coverage of streams and rivers (0.42 % for stream order 4) corresponds to the global average of 0.47 % (Raymond et al., 2013) and also mean terrestrial NPP in the catchments ($515\,g\,C\,m^{-2}\,yr^{-1}$) was in close correspondence to recent global mean estimates ($495\,g\,C\,m^{-2}\,yr^{-1}$; Zhao et al., 2005).

By combining CO_2 evasion and downstream C-export by stream discharge, we estimated that $13.9\,g\,C\,m^{-2}\,yr^{-1}$, corresponding to 2.7 % of terrestrial NPP, are exported from the catchments by streams and rivers, in which both evasion and discharge contributed equally to this flux. Also, these findings are in close agreement with global and continental-scale estimates of 16 and $13.5\,g\,C\,m^{-2}\,yr^{-1}$, respectively (Table 3).

4.3 Aquatic C-export across spatial scales

Although not exhaustive, Table 3 provides data from a large share of existing studies relating the aquatic C-export to terrestrial production in the corresponding catchments, which cover a broad range of spatial scales and different landscapes. Except for the tropical forest of the Amazon basin, the aquatic C-export normalized to catchment area estimated for temperate streams in our study is surprisingly similar to those estimated at comparable and at larger spatial scale. In the Amazon, the fraction of terrestrial production that is exported by the fluvial network is more than 2-fold higher (nearly 7 % of NPP; Richey et al., 2002). However, it must be noted that a large fraction of the regional NPP in the Amazon is supported by aquatic primary production by macrophytes and C export is predominantly controlled by wetland connectivity, with wetlands covering up to 14 % of the land surface area (Abril et al., 2013). An additional peculiarity of the Amazon is that, in contrast to the remaining systems, the vast majority (87 %) of the total C-export is governed by CO_2 evasion (Table 3), whereas lateral export constitutes a much smaller component. An exceptionally low fraction of NPP that is exported from aquatic systems at larger scale was estimated for the English Lake District (1.6 %; Maberly et al., 2013), though only CO_2 evasion from lake surfaces was considered, i.e., downstream discharge by rivers was ignored. Their estimate agrees reasonably well with the fraction of catchment NPP that was emitted to the atmosphere from the stream network in the present study (1.3 %). If a similar share of catchment NPP was also exported with river discharge in the Lake District, the average mass of C exported from the aquatic systems per unit catchment area would be in close agreement with our and other larger-scale estimates (Table 3).

In more detailed studies at smaller scales and for individual catchments, aquatic C-export was exclusively related to net ecosystem exchange (NEE) measured by eddy covariance. Here, the estimated fractions of aquatic export range between 2 % of NEE in a temperate forest catchment (only discharge, evasion not considered; Shibata et al., 2005) and 160 % of NEE in a boreal peatland catchment (Billett et al., 2004). Analysis of interannual variations in stream export from a small peatland catchment in Sweden (Leach et al., 2016) resulted in estimates of C export by the fluvial network between 5.9 and $18.1\,g\,C\,m^{-2}\,yr^{-1}$ over 12 years. The total mean value of $12.2\,g\,C\,m^{-2}\,yr^{-1}$, however, is in close agreement with the present and other larger-scale estimates (Table 3). In contrast to the present study, C export from the peatland catchments was dominated by stream discharge of DIC.

4.4 Controlling factors for aquatic C-export

We found a significant linear relationship between total catchment NPP and the C export from the catchment in the stream network across 4 Strahler orders. The relationship was mainly caused by a strong correlation between catchment size and water surface area. As expected for temperate zones, large streams and rivers with large surface area have larger catchments. A study analyzing aquatic C-fluxes for 18 hydrological units in the conterminous US (Butman et al., 2015) observed a significant correlation between catchment-specific aquatic C yield and specific catchment NEP, which in turn was linearly correlated to NPP. We did not observe such a correlation at smaller scale, which could be related to the rather narrow range of variability in NPP among the considered catchments. Nevertheless, the linear correlation observed by Butman et al. (2015) indicates that a constant fraction of terrestrial NPP is exported by aquatic systems if averaged over larger spatial scales.

The relatively narrow range of variability in C export per catchment area (between 9 and $18\,g\,C\,m^{-2}\,yr^{-1}$, with the two exceptions discussed above) in different landscapes (Table 3) is rather surprising. Although this range of variation is most likely within the uncertainty of the various estimates, the variability across different landscapes is certainly small in comparison to the order of magnitude differences in potential controlling factors like catchment NPP, fractional water coverage as well as size and climatic zone of the study area. In lake-rich regions, evasion from inland waters was observed to be dominated by lakes (Buffam et al., 2011; Jonsson et al., 2007), which cover up to 13 % of the surface area of those regions. In the present study, as well as in other studies on catchments where lakes are virtually absent (Wallin et al., 2013) and the fractional water coverage was smaller than 0.5 % of the terrestrial surface area, an almost identical

Table 3. Summary of estimates of aquatic C-export in relation to terrestrial production in the watershed across different spatial scales (spatial scale decreases from top to bottom). Aquatic C-export is the sum of C-discharge and evasion (numbers in parentheses also include the change in C storage in the aquatic systems by sedimentation) normalized by the area of the terrestrial watershed. Aquatic C fate refers to the percentage of the total exported C which is emitted to the atmosphere (evasion) and transported downstream (discharge). The missing percentage is the fraction which is stored in the aquatic systems by sedimentation (if considered). Terrestrial production is expressed as NPP or as net ecosystem exchange (NEE). n.c. indicates that this compartment/flux was not considered in the respective study.

Study area (catchment size in km^2)	Fractional water coverage (%) rivers: R lakes: L	Aquatic C export ($g\,C\,m^{-2}\,yr^{-1}$)	Aquatic C fate (%): evasion: E discharge: D	Aquatic C-export/ terrestrial production (%) NPP	NEE	Reference
Global (1.3×10^8)	R: 0.2–0.3 L: 2.1–3.4	16 (20)	E: 44 D: 34	3.7[1]	21–64[2]	Aufdenkampe et al. (2011)
Conterminous US (7.8×10^6)	R: 0.52 L: 1.6	13.5 (18.8)	E: 58 D: 28	3.6	27[3]	Butman et al. (2015)
Central Amazon (1.8×10^6)	4–16	138 D: 13	E: 87	6.8[4]	n.c.	Richey et al. (2002)
Yellow River network (7.5×10^5)	R: 0.3–0.4 L: n.c.	18.5 (30)	E: 35 D: 26	n.c.	96 (62)	Ran et al. (2015)
North temperate lake district (6400)	R: 0.5 L: 13	11.8 (16)	E: 33 D: 41	n.c.	7	Buffam et al. (2011)
Northern Sweden (peat) (3025)	R: 0.33 L: 3.5	9	E: 50 (4.5) D: 50 (4.5)	n.c.	6	Jonsson et al. (2007)
Temperate streams (0.7–1227)	R: 0.33 L: n.c.	13.9	E: 47 D: 53	2.7	n.c.	This study
English Lake district (1–360)	R: n.c. L: 2.2	5.4	E: 100 D: n.c.	1.6	n.c.	Maberly et al. (2013)
Forested stream catchments in Sweden (0.46–67)	R: 0.1–0.7 L: n.c. (<0.7)	9.4	E: 53 D: 47	n.c.	8–17	Wallin et al. (2013)
Forest catchment in Japan (9.4)	R: – L: n.c.	4	E: n.c. D: 100	n.c.	2	Shibata et al. (2005)
Peatland catchment (3.35)	R: 0.05 L: n.c.	30.4	E: 13 D: 87	n.c.	160	Billett et al. (2004)
Peatland catchment (2.7)	R: n.c. L: 2.2	12.2	E: – D: –	n.c.	12–50	Leach et al. (2016)

[1] For a value of $56\,Pg\,C\,yr^{-1}$ for global NPP (Zhao et al., 2005).
[2] Global mean NEE was estimated as the difference of gross primary production (GPP) and ecosystem respiration, which was assumed to be 91–97 % of GPP (Randerson et al., 2002).
[3] This percentage refers to NEP instead of NEE.
[4] For a global mean value of NPP in tropical forests of $1148\,g\,C\,m^{-2}\,yr^{-1}$ (Sabine et al., 2004).

catchment-specific C export and evasion rate has been observed (Table 3). CO_2 emissions from water surfaces depend on the partial pressure of CO_2 in water and are therefore related to DIC, which was the dominant form of dissolved C in the present study. Studies in the boreal zone, where dissolved C in the aquatic systems is mainly in the form of DOC, however, found comparable catchment-specific C export and evasion rates (Leach et al., 2016; Jonsson et al., 2007; Wallin et al., 2013; cf. Table 3). The difference in the speciation of the exported C indicates that a larger fraction of the terrestrial NPP is respired by heterotrophic respiration in soils and exported to the stream network as DIC in the present study, in contrast to export as DOC and predominantly aquatic respiration. Observations and modeling of terrestrial–aquatic C fluxes across the US suggested a transition in the source of aquatic CO_2 from direct terrestrial input to aquatic CO_2 production by degradation of terrestrial organic C with increasing stream size (Hotchkiss et al., 2015). Such a transition

was not observed in the present study, where organic C made a small contribution to the fluvial C-load across all investigated stream orders. In addition to soil respiration, mineral weathering also contributes to DIC in stream water. The relative importance of soil respiration and weathering varies depending on geology and the presence of wetlands in the area (Hotchkiss et al., 2015; Lauerwald et al., 2013; Jones et al., 2003). In the present study, 16 % of the catchment areas contained carbonate bedrock. The DIC concentration in the water increased with the proportion of carbonate containing bedrock in the catchment ($R^2 = 0.33$, $p < 0.001$).

Despite the small number of observations in the meta-analysis, the narrow range of variability in C export per catchment area may indicate that neither water surface area nor the location of mineralization of terrestrial derived C (soil respiration and export of DIC versus export of DOC and mineralization in the aquatic environment) are important drivers for the total C-export from catchments by inland waters at larger spatial scales. This rather unexpected finding deserves further attention, as it suggests that other, currently poorly explored, processes control the aquatic–terrestrial coupling and the role of inland waters in regional C-cycling. Given the significant contribution of inland waters to regional and global-scale greenhouse gas emissions, the mechanistic understanding of these processes is urgently required to assess their vulnerability to ongoing climatic and land use changes, as well as to the extensive anthropogenic influences on freshwater ecosystems. Recent developments of process-based models, which are capable of resolving the boundless biogeochemical cycle in the terrestrial–aquatic continuum from catchment to continental scales (Nakayama, 2016), are certainly an important tool for these future studies.

5 Conclusions

Our analysis of the C budget in a temperate stream network on a regional scale revealed a relationship between aquatic C-export and terrestrial NPP. On average, 13.9 g C m^{-2} yr^{-1}, corresponding to 2.7 % of the terrestrial NPP, were exported from the catchments by rivers and streams with CO_2 evasion and downstream transport contributing equally to the export. A comparison of our regional-scale study with other studies from different scales and landscapes showed a relatively narrow range of variability in C export per catchment area. Future research is needed to understand the processes that control the aquatic–terrestrial coupling and the role of inland waters in regional C-cycling.

Data availability. Underlying data are available in the Supplement.

The Supplement related to this article is available online at https://doi.org/10.5194/bg-14-5003-2017-supplement.

Competing interests. The authors declare that they have no conflict of interest.

Acknowledgements. This study was financially supported by the German Research Foundation (grant no. LO 1150/9-1). We thank Miriam Tenhaken for contributing to a preliminary analysis. All raw data for this paper are properly cited and referred to in the reference list. The processed data, which were used to generate the figures and tables, are available upon request to the corresponding author.

Edited by: Minhan Dai
Reviewed by: Lishan Ran and two anonymous referees

References

Abril, G., Martinez, J.-M., Artigas, L. F., Moreira-Turcq, P., Benedetti, M. F., Vidal, L., Meziane, T., Kim, J.-H., Bernardes, M. C., Savoye, N., Deborde, J., Souza, E. L., Alberic, P., Landim de Souza, M. F., and Roland, F.: Amazon River carbon dioxide outgassing fuelled by wetlands, Nature, 505, 395–398, https://doi.org/10.1038/nature12797, 2013.

Abril, G., Bouillon, S., Darchambeau, F., Teodoru, C. R., Marwick, T. R., Tamooh, F., Ochieng Omengo, F., Geeraert, N., Deirmendjian, L., Polsenaere, P., and Borges, A. V.: Technical Note: Large overestimation of pCO_2 calculated from pH and alkalinity in acidic, organic-rich freshwaters, Biogeosciences, 12, 67–78, https://doi.org/10.5194/bg-12-67-2015, 2015.

Aufdenkampe, A. K., Mayorga, E., Raymond, P. A., Melack, J. M., Doney, S. C., Alin, S. R., Aalto, R. E., and Yoo, K.: Riverine coupling of biogeochemical cycles between land, oceans, and atmosphere, Front. Ecol. Environ., 9, 53–60, https://doi.org/10.1890/100014, 2011.

Barros, N., Cole, J. J., Tranvik, L. J., Prairie, Y. T., Bastviken, D., Huszar, V. L. M., del Giorgio, P., and Roland, F.: Carbon emission from hydroelectric reservoirs linked to reservoir age and latitude, Nat. Geosci., 4, 593–596, https://doi.org/10.1038/ngeo1211, 2011.

Battin, T. J., Luyssaert, S., Kaplan, L. A., Aufdenkampe, A. K., Richter, A., and Tranvik, L. J.: The boundless carbon cycle, Nat. Geosci., 2, 598–600, https://doi.org/10.1038/ngeo618, 2009.

Billett, M. F., Palmer, S. M., Hope, D., Deacon, C., Storeton-West, R., Hargreaves, K. J., Flechard, C., and Fowler, D.: Linking land-atmosphere-stream carbon fluxes in a lowland peatland system, Global Biogeochem. Cy., 18, GB1024, https://doi.org/10.1029/2003GB002058, 2004.

Buffam, I., Turner, M. G., Desai, A. R., Hanson, P. C., Rusak, J. A., Lottig, N. R., Stanley, E. H., and Carpenter, S. R.: Integrating aquatic and terrestrial components to construct a complete carbon budget for a north temperate lake district, Global Change Biol., 17, 1193–1211, https://doi.org/10.1111/j.1365-2486.2010.02313.x, 2011.

Butman, D. and Raymond, P. A.: Significant efflux of carbon dioxide from streams and rivers in the United States, Nat. Geosci., 4, 839–842, 2011.

Butman, D., Stackpoole, S., Stets, E., McDonald, C. P., Clow, D. W., and Striegl, R. G.: Aquatic carbon cycling

in the conterminous United States and implications for terrestrial carbon accounting, P. Natl. Acad. Sci., 58–63, https://doi.org/10.1073/pnas.1512651112, 2015.

Christensen, T. R., Johansson, T., Olsrud, M., Ström, L., Lindroth, A., Mastepanov, M., Malmer, N., Friborg, T., Crill, P., and Callaghan, T. V.: A catchment-scale carbon and greenhouse gas budget of a subarctic landscape, Philos. T. Roy. Soc. A, 365, 1643–1656, https://doi.org/10.1098/rsta.2007.2035, 2007.

Cole, J. J., Prairie, Y. T., Caraco, N. F., McDowell, W. H., Tranvik, L. J., Striegl, R. G., Duarte, C. M., Kortelainen, P., Downing, J. A., Middelburg, J. J., and Melack, J.: Plumbing the global carbon cycle: Integrating inland waters into the terrestrial carbon budget, Ecosystems, 10, 171–184, https://doi.org/10.1007/s10021-006-9013-8, 2007.

DIN EN ISO 9963-1:1996-02: Wasserbeschaffenheit – Bestimmung der Alkalinität – Teil 1: Bestimmung der gesamten und der zusammengesetzten Alkalinität (ISO 9963-1:1994); German version EN ISO 9963-1:1995, 1996.

DIN EN ISO 9963-2:1996-02: Wasserbeschaffenheit – Bestimmung der Alkalinität – Teil 2: Bestimmung der Carbonatalkalinität (ISO 9963-2:1994); German version EN ISO 9963-2:1995, 1996.

DIN EN ISO 10523:2012-04: Wasserbeschaffenheit – Bestimmung des pH-Werts (ISO 10523:2008); German version EN ISO 10523:2012, 2012.

EEA: Corine Land Cover 2006 seamless vector data, European Environment Agency, https://www.eea.europa.eu/data-and-maps/data/clc-2006-vector-4, last access: 2 November 2017, 2006.

Hotchkiss, E. R., Hall Jr., R. O., Sponseller, R. A., Butman, D., Klaminder, J., Laudon, H., Rosvall, M., and Karlsson, J.: Sources of and processes controlling CO_2 emissions change with the size of streams and rivers, Nat. Geosci., 8, 696–699, https://doi.org/10.1038/ngeo2507, 2015.

Jones, J. B., Stanley, E. H., and Mulholland, P. J.: Long-term decline in carbon dioxide supersaturation in rivers across the contiguous United States, Geophys. Res. Lett., 30, 1495, 2003.

Jonsson, A., Algesten, G., Bergström, A. K., Bishop, K., Sobek, S., Tranvik, L. J., and Jansson, M.: Integrating aquatic carbon fluxes in a boreal catchment carbon budget, J. Hydrol., 334, 141–150, https://doi.org/10.1016/j.jhydrol.2006.10.003, 2007.

Lauerwald, R., Hartmann, J., MooSDorf, N., Kempe, S., and Raymond, P. A.: What controls the spatial patterns of the riverine carbonate system? – A case study for North America, Chem. Geol., 337, 114–127, 2013.

Lauerwald, R., Laruelle, G. G., Hartmann, J., Ciais, P., and Regnier, P. A.: Spatial patterns in CO2 evasion from the global river network, Glob. Biogeochem. Cy., 29, 534–554, 2015.

Leach, J. A., Larsson, A., Wallin, M. B., Nilsson, M. B., and Laudon, H.: Twelve year interannual and seasonal variability of stream carbon export from a boreal peatland catchment, J. Geophys. Res.-Biogeo., 121, 1851–1866, https://doi.org/10.1002/2016JG003357, 2016.

Leopold, L. B. and Maddock Jr., T.: The hydraulic geometry of stream channels and some physiographic implications2330-7102, 1953.

LVermGeoRP: Vermessungs- und Katasterverwaltung Rheinland-Pfalz, Landesamt für Vermessung und Geobasisinformation Rheinland-Pfalz, 2012.

Maberly, S. C., Barker, P. A., Stott, A. W., and De Ville, M. M.: Catchment productivity controls CO_2 emissions from lakes, Nat. Clim. Chang., 3, 391–394, https://doi.org/10.1038/nclimate1748, 2013.

MULEWF: GeoPortal Wasser, Ministerium für Umwelt, Landwirtschaft, Ernährung, Weinbau und Forsten Rheinland-Pfalz, 2013.

MULEWF: Wasserwirtschaftsverwaltung Rheinland-Pfalz, Ministerium für Umwelt, Landwirtschaft, Ernährung, Weinbau und Forsten Rheinland-Pfalz, 2015.

Nakayama, T.: New perspective for eco-hydrology model to constrain missing role of inland waters on boundless biogeochemical cycle in terrestrial–aquatic continuum, Ecohydrology & Hydrobiology, 16, 138–148, https://doi.org/10.1016/j.ecohyd.2016.07.002, 2016.

Parkhurst, D. L. and Appelo, C.: User's guide to PHREEQC (Version 2): A computer program for speciation, batch-reaction, one-dimensional transport, and inverse geochemical calculations, 1999.

R Development Core Team: R: A language and environment for statistical computing, R Foundation for Statistical Computing, Vienna, Austria, 2011.

Ran, L., Lu, X. X., Yang, H., Li, L., Yu, R., Sun, H., and Han, J.: CO_2 outgassing from the Yellow River network and its implications for riverine carbon cycle, J. Geophys. Res.-Biogeo., 120, 1334–1347, https://doi.org/10.1002/2015JG002982, 2015.

Randerson, J. T., Chapin, F. S., Harden, J. W., Neff, J. C., and Harmon, M. E.: Net ecosystem production: a comprehensive measure of net carbon accumulation by ecosystems, Ecol. Appl., 12, 937–947, https://doi.org/10.1890/1051-0761(2002)012[0937:NEPACM]2.0.CO;2, 2002.

Raymond, P. A., Oh, N.-H., Turner, R. E., and Broussard, W.: Anthropogenically enhanced fluxes of water and carbon from the Mississippi River, Nature, 451, 449–452, 2008.

Raymond, P. A., Zappa, C. J., Butman, D., Bott, T. L., Potter, J., Mulholland, P., Laursen, A. E., McDowell, W. H., and Newbold, D.: Scaling the gas transfer velocity and hydraulic geometry in streams and small rivers, Limnol. Oceanogr., 2, 41–53, 2012.

Raymond, P. A., Hartmann, J., Lauerwald, R., Sobek, S., McDonald, C., Hoover, M., Butman, D., Striegl, R., Mayorga, E., Humborg, C., Kortelainen, P., Durr, H., Meybeck, M., Ciais, P., and Guth, P.: Global carbon dioxide emissions from inland waters, Nature, 503, 355–359, https://doi.org/10.1038/nature12760, 2013.

Richey, J. E., Melack, J. M., Aufdenkampe, A. K., Ballester, V. M., and Hess, L. L.: Outgassing from Amazonian rivers and wetlands as a large tropical source of atmospheric CO_2, Nature, 416, 617–620, https://doi.org/10.1038/416617a, 2002.

Running, S. W., Nemani, R. R., Heinsch, F. A., Zhao, M., Reeves, M., and Hashimoto, H.: A Continuous Satellite-Derived Measure of Global Terrestrial Primary Production, Bioscience, 54, 547–560, https://doi.org/10.1641/0006-3568(2004)054[0547:acsmog]2.0.co;2, 2004.

Sabine, C. L., Heimann, M., Artaxo, P., Bakker, D. C., Chen, C.-T. A., Field, C. B., Gruber, N., Le Quéré, C., Prinn, R. G., and Richey, J. E.: Current status and past trends of the global carbon cycle, in: The Global Carbon Cycle, 2nd ed., edited by: Field, C. B. and Raupach, M. R., Scientific Committee on Problems of the Environment (SCOPE) Series, Island Press, 17–44, 2004.

Shibata, H., Hiura, T., Tanaka, Y., Takagi, K., and Koike, T.: Carbon cycling and budget in a forested basin of south-

western Hokkaido, northern Japan, Ecol. Res., 20, 325–331, https://doi.org/10.1007/s11284-005-0048-7, 2005.

Stanley, E. H., Casson, N. J., Christel, S. T., Crawford, J. T., Loken, L. C., and Oliver, S. K.: The ecology of methane in streams and rivers: patterns, controls, and global significance, Ecol. Monogr., 146–171, 2016.

Statistisches Landesamt Rheinland-Pfalz: Statistisches Jahrbuch 2014, Statistisches Landesamt Rheinland-Pfalz, Bad Ems, 2014.

Strahler, A. N.: Quantitative analysis of watershed geomorphology, Eos, Transactions American Geophysical Union, 38, 913–920, 1957.

Stumm, W. and Morgan, J. J.: Aquatic chemistry: chemical equilibria and rates in natural waters, Wiley, 3rd Edition, New York, 1996.

Tranvik, L. J., Downing, J. A., Cotner, J. B., Loiselle, S. A., Striegl, R. G., Ballatore, T. J., Dillon, P., Finlay, K., Fortino, K., Knoll, L. B., Kortelainen, P. L., Kutser, T., Larsen, S., Laurion, I., Leech, D. M., McCallister, S. L., McKnight, D. M., Melack, J. M., Overholt, E., Porter, J. A., Prairie, Y., Renwick, W. H., Roland, F., Sherman, B. S., Schindler, D. W., Sobek, S., Tremblay, A., Vanni, M. J., Verschoor, A. M., von Wachenfeldt, E., and Weyhenmeyer, G. A.: Lakes and reservoirs as regulators of carbon cycling and climate, Limnol. Oceanogr., 54, 2298–2314, https://doi.org/10.4319/lo.2009.54.6_part_2.2298, 2009.

Wallin, M. B., Grabs, T., Buffam, I., Laudon, H., Ågren, A., Öquist, M. G., and Bishop, K.: Evasion of CO_2 from streams – The dominant component of the carbon export through the aquatic conduit in a boreal landscape, Glob. Change Biol., 19, 785–797, https://doi.org/10.1111/gcb.12083, 2013.

Walvoord, M. A. and Striegl, R. G.: Increased groundwater to stream discharge from permafrost thawing in the Yukon River basin: Potential impacts on lateral export of carbon and nitrogen, Geophys. Res. Lett., 34, L12402, 2007.

Zhang, W. and Montgomery, D. R.: Digital elevation model grid size, landscape representation, and hydrologic simulations, Water Resour. Res., 30, 1019–1028, https://doi.org/10.1029/93WR03553, 1994.

Zhao, M., Heinsch, F. A., Nemani, R. R., and Running, S. W.: Improvements of the MODIS terrestrial gross and net primary production global data set, Remote Sens. Environ., 95, 164–176, https://doi.org/10.1016/j.rse.2004.12.011, 2005.